Traffic Sign Segmentation in Natural Scenes Based on Color and Shape Features

Qiong Wang
School of Computer Science and Engineering
Nanjing University of Science and Technology, Nanjing, China
wangq@njust.edu.cn

Xinxin Liu
School of Computer Science and Engineering,
Nanjing University of Science and Technology, Nanjing, China
lxinxin20082008@163.com

***Abstract*—Traffic sign detection and recognition is one of the important fields in the intelligent transportation system, and is expected to provide information on traffic signs and guide vehicles during driving. Traffic sign segmentation is the first stage in traffic sign recognition system, and segmentation results influence the recognition results. This paper presents an efficient method for traffic sign segmentation in natural scenes. Firstly, the improved RGB color space is presented to obtain the initial segmentation and get the ROI in the image. Then the contour features are extracted in the binary image for moment invariants calculation. Finally, traffic signs are segmented according to the color and shape features. Experiments with a large dataset and comparison with other approaches show the robustness and accuracy of the method.**

Keywords-component; traffic sign segmentation; improved RGB color space; moment invariants based on boundary; shape feature

I. INTRODUCTION

Traffic signs detection and recognition is a subsystem of the intelligent transportation system [1]. It can be applied in driver assistance systems and unmanned vehicles. A full traffic signs recognition system is composed of two main stages, detection and recognition. The goal of the first stage is to identify potential traffic signs in the image, i.e. the possible regions that represent road signs characteristics, using either color or shape information. In the second stage, the potential regions are further analyzed to determine the correct sign and its meaning.

Existing traffic signs segmentation algorithm can be roughly divided into three categories: feature space-based segmentation [2-7]; image domain-based segmentation [8-10] and feature extraction and color clustering-based segmentation [11-14].

In order to improve the segmentation accuracy, the color and shape feature of traffic signs are comprehensively considered for segmentation. Some segmentation algorithms only fit for to certain types of traffic signs, and are lack of generality [15]. The proposed method can be adapted to the existing traffic signs, and can achieve effective segmentation under complex scene. First, the image is segmented in the normalized RGB color space in order to reduce the impact of lighting conditions, while the chromatic/achromatic model is introduced to the normalized RGB space [16]. Then, the segmentation image is converted to grayscale and binary image. Thirdly, contour feature is extracted from the binary image and represented by chain code. Finally, precise segmentation is obtained according to the boundary invariant moment.

II. INITIAL SEGMENTATION BASED ON COLOR FEATURE

It is possible to remove most of the non-target region after segmentation by color feature.

RGB space is the basic color space, and it is the initial color space of a camera to capture. Any color can be obtained through the calculation in RGB space model. So when the light condition changes, it is difficult to achieve precise segmentation. Therefore, we use the normalized RGB model to solve this problem. The three components were normalized to *R', G', B'*, and *R'+G'+B'* = 1. The normalized RGB expression is defined as:

$$\begin{aligned} R' &= R/(R+G+B) \\ G' &= G/(R+G+B) \\ B' &= B/(R+G+B) \end{aligned} \tag{2.1}$$

For the three types of traffic signs, their color features are red, blue and yellow. A single component histogram value and experience value can be determined for each type of the range. However, some white-color areas and non-color areas are also preserved, which are need to solve with do achromatic model [16].

This paper proposed an improved RGB space by introducing the achromatic model the normalized RGB space. Achromatic model is shown in equation (2.2), where D is the achromatic extraction degrees, and the value of D is 30.

$$CAD(R,G,B) = \frac{(|R-G|+|G-B|+|B-R|)}{3D} \tag{2.2}$$

For any pixel in the image, take it into the equation (2.2). If the calculation result is less than or equal to 1, it can be considered as an achromatic pixel.

Figure 1 shows the original color images with traffic signs, which contain single or multiple traffic signs.

Figure 2 shows the segmentation results in normalized RGB space.

Figure 3 shows the segmentation results in improved RGB space. The experiments demonstrate that the traffic signs can be segmented effectively by using the achromatic model in normalized RGB space.

978-1-4799-6989-0/14/$31.00©2014 IEEE

Figure 1. Original images.

Figure 2. Segmentation results in normalized RGB space.

Figure 3. Segmentation results in improved RGB space.

III. SEGMENTATION BASED ON SHAPE FEATURES

The initial segmentation images which are processed by using color features are converted to gray scale images, and the pixels of most non-target regions are set to be 0. Corresponds to the highest peak in the histogram, a threshold is set to output binary images. Then morphological closing operation is processed, it can connect small broken region and extract the contour. The final shape is discriminated according to the contour extraction and the chain code, which o achieve the goal of accurate segmentation.

A. Moment Invariants Baesd on Target Boundary

Moment invariants have been frequently used as features for shape discrimination. They are computed based on the information provided by both the shape boundary and its interior region. The moment invariants based on target boundary was proposed as the improved moment invariants computed using the shape boundary only, which tremendously reduces computations. [18]

For continuous curve C, define the (p, q)th moment as:

$$m_{p,q} = \int_C x^p y^q ds \ , \text{ where } p, q = 0,1,2\ldots \tag{3.1}$$

$ds = \sqrt{(dx)^2 + (dy)^2}$, the modified central moments can be similarly defined as equation (3.2):

$$\mu_{p,q} = \int_C (x-\bar{x})^p (y-\bar{y})^q ds, \ \bar{x} = \frac{m_{1,0}}{m_{0,0}}, \bar{y} = \frac{m_{0,1}}{m_{0,0}} \tag{3.2}$$

For a digital shape, equation (3.2) becomes

$$\mu_{p,q} = \sum_{(x,y)\in C} (x-\bar{x})^p (y-\bar{y})^q \tag{3.3}$$

The modified central moments are invariant to translation. The modified central moments can be normalized by using equation (3.4) such that they are also scaling-invariant, and provide an alternative and intuitive proof of rotation invariance for the improved moment invariants.

$$\eta_{p,q} = \frac{\mu_{p,q}}{\mu_{0,0}^{p+q+1}} \text{, where } p+q = 2,3\ldots \tag{3.4}$$

Use ϕ_i to represent the *i-th* moment invariants, then equation (3.5) are given as follows:

$$\begin{aligned}
&\phi_1 = \eta_{2,0} + \eta_{0,2}\ , \qquad \phi_2 = (\eta_{2,0} - \eta_{0,2})^2 + 4\eta_{1,1} \\
&\phi_3 = (\eta_{3,0} - 3\eta_{1,2})^2 + (\eta_{0,3} - 3\eta_{2,1})^2 \\
&\phi_4 = (\eta_{3,0} + \eta_{1,2})^2 + (\eta_{0,3} + \eta_{2,1})^2 \\
&\phi_5 = (\eta_{3,0} - 3\eta_{1,2})(\eta_{3,0} + \eta_{1,2})[(\eta_{3,0} + \eta_{1,2})^2 - \\
&\quad 3(\eta_{2,1} + \eta_{0,3})^2] + (3\eta_{2,1} - \eta_{0,3})(\eta_{2,1} + \eta_{0,3})[3(\eta_{3,0} + \eta_{1,2})^2 - (\eta_{2,1} + \eta_{0,3})^2] \\
&\phi_6 = (\eta_{2,0} - \eta_{0,2})[(\eta_{3,0} + \eta_{1,2})^2 - (\eta_{2,1} + \eta_{0,3})^2] + 4\eta_{1,1}(\eta_{3,0} + \eta_{1,2})(\eta_{0,3} + \eta_{2,1}) \\
&\phi_7 = (3\eta_{2,1} - \eta_{0,3})(\eta_{3,0} + \eta_{1,2})[(\eta_{3,0} + \eta_{1,2})^2 \\
&\quad - 3(\eta_{2,1} + \eta_{0,3})^2] + (3\eta_{1,2} - \eta_{3,0})(\eta_{2,1} + \eta_{0,3})[3(\eta_{3,0} + \eta_{1,2})^2 - (\eta_{2,1} + \eta_{0,3})^2]
\end{aligned} \tag{3.5}$$

For rotation invariance, the curve C can be assumed by a certain angle of rotation to obtain the curve C'. Using trigonometric identity as follows can prove that seven moment invariants in equation (3.5) still hold.

$$\cos^2\theta + \sin^2\theta = 1$$

$$(\cos^3\theta - 3\cos\theta\sin^2\theta)^2 + (\sin^3\theta - 3\sin\theta\cos^2\theta)^2 = 1$$

Since the moment invariants based on target boundary can effectively detect the shape and are invariant to scaling, translation, and rotation. We can use them to determine the shape of traffic signs. The shapes of traffic signs include round, triangle, rectangle, and octagon, as shown in Figure4.

Figure 4. Part of the traffic signs template images.

B. Accurate Traffic Signs Segmentation

The moment invariants of each standard traffic sign are calculated to establish standard templates of moment invariants. Specifically, the moment invariants of the same type traffic signs with different size and different rotation angle are calculated and then the average values of those moment invariants are the final template for each shape. Finally, the accurate traffic signs segmentation can be achieved by using template matching.

Through calculating the a large number of template traffic sign images, the moment invariants values for different shapes of traffic signs are given in the Table 1.

TABLE I. TEMPLATE IMAGES' MOMENT INVARIANTS BASED ON BOUNDARY

Shape	Moment Invariants Based on Boundary						
	$\phi_1'_{\perp}$	$\phi_2'_{\perp}$	$\phi_3'_{\perp}$	$\phi_4'_{\perp}$	$\phi_5'_{\perp}$	$\phi_6'_{\perp}$	$\phi_7'_{\perp}$
Circle	1.5096	6.8151	9.5229	9.5000	19.0483	13.1677	19.6521
Octagon	1.6818	7.6458	9.5214	9.6867	19.2508	14.1594	20.4682
Triangle	1.6562	6.8532	5.9041	7.8956	14.8003	11.4473	16.5146
Square	1.6831	7.9309	9.7616	10.6346	20.9849	15.0441	22.0009
Rectangle	1.6580	4.2496	9.1139	9.6680	19.2847	11.8538	19.5094

For any traffic sign image under natural scene, its moment invariants based on boundary $(\phi_1, \phi_2, \phi_3, \phi_4, \phi_5, \phi_6, \phi_7)$ is calculated. Then the moment invariants values are compared with the values in Table 1 by equation (3.6) to determine whether this region is the traffic sign region or not.

$$Sum = \sum_{i=1}^{7} (\phi_i - \phi_i')^2, \ if\ Sum < \mathrm{T}, \text{ is sign region} \qquad (3.6)$$

If the equation (3.6) holds, this region is the traffic signs region. Experimental results show it can accurately determine the shape and remove non-traffic sign area if T is 6. If T is more than 6, indicate that it is non-traffic sign region. Furthermore, the categories of traffic signs can also be determined by using this method. The shape of the minimum Sum value is corresponding to the template image in Table1.

C. *Experiments on Natural Scene Images*

The complex scenes contain a variety of factors which increase the difficulty of traffic sign segmentation, such as the natural light change due to the time of day, the weather change, sign occlusion and etc. .

In this paper, the method for traffic signs segmentation under the complicated natural scenes can tolerant a certain degree of shape change by setting the sum of squares of differences of the template shapes and target region. So effective segmentation results can still be obtained in spite of or partial occlusion shades, color fading, and shape distortion. In general, it can get the traffic sign region in the final segmentation correctly as long as the closed contours can be obtained by using color characteristics to segment sign regions initially.

Figure 5 to Figure8 show the effectiveness of our method under different scenes. This method is robust to a certain degree of deformation and occlusion.

To evaluate the performance of the proposed road signs segmentation method, we do experiments on the real road scenes images and the segmentation results shown in Figure 9. The experimental results also show that this method is effective to segment traffic signs in complicated natural scenes.

(a) Original image (b) Segmentation result

Figure 5. Multiple traffic signs.

(a) Original image (b) Segmentation result

Figure 6. Traffic signs with shadow.

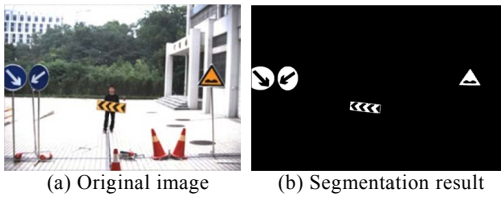

(a) Original image (b) Segmentation result

Figure 7. Traffic sign has tilt angle.

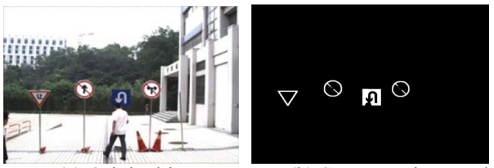

(a) Original image (b) Segmentation result

Figure 8. Traffic signs with partial occlusion.

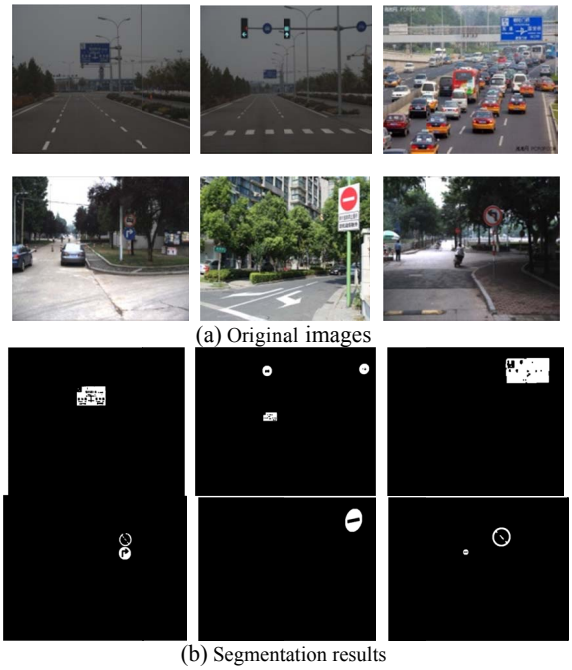

(a) Original images

(b) Segmentation results

Figure 9. Traffic sign segmentation in natural scenes.

The performance of our methods is compared with other sign segmentation methods. In paper [5], HSV color space is used for initial segmentation, and the contour transformation characteristics are extracted to train SVM classifier for shape discrimination. In paper [6], the normalized RGB color space is also used to segmentation, and then the geometrical characteristics of the traffic signs are used for shape discrimination. The comparison results are shown in Table 2. Correct number denotes the number of images in which the traffic signs are correctly segmented. False-alarm number is the number of images in which the noise objects are wrongly segmented as traffic signs. Miss number is the numbers of images in which traffic signs are missed.

As can be seen in table 2, the segmentation result of our method is similar with the method in paper [5]. But the complexity of the algorithm in paper [5] is high and cost more running time than ours.

IV. CONCLUSIONS

In this paper, an efficient and robust traffic signs segmentation method based on color and shape information is proposed. The method is based on normalized RGB space and moment invariants. We proposed an efficient segmentation method and experiments with natural road images show that the proposed method is particularly robust against severe illumination changes for images taken under various conditions. Comparison with other approaches based on color information show that the proposed method achieves the good segmentation results while requiring the least computation time. The simplicity and the robustness of the method make it suitable for real-time applications such as on-board driver assistance systems and unmanned vehicles. Our future works include using the proposed method as a first step of a sign recognition system.

ACKNOWLEDGMENT

This work was financially supported by the Jiangsu Key Laboratory of Image and Video Understanding for Social Safety (Nanjing University of Science and Technology), Grant No. 30920140122007, and the Priority Academic Program Development of Jiangsu Higher Education Institutions (PAPD).

REFERENCES

[1] H. Gerland. ITS intelligent transportation system: fleet management with GPS dead reckoning, advanced displays , smartcards[c]. IEEE-IEE Vehicle Navigation & Information Systems conference. Ottawa, Canada, 1993, 606~611

[2] V. Andrey, J. Kang Hyun. Road guidance sign recognition in urban areas by structure[C]. Strategic Technology, 2006,pp:293-296

[3] A.de la Escalera, J. Armingol, J. Pastor,et al, Visual sign information extraction and identification by deformable models for intelligent vehicles[J].Intelligent Transportation Systems, 2004,5(20:57-68

[4] F. Ren, J. Huang, R. Jian, General traffic sign recognition by feature matching[C]. Image and Vision Computing, New Zealand, 2009,pp:409-414

[5] Z. Usman, A.E. Eran, H. Amir. Road Sign Detection and Recognition from Video Stream Using HSV, Contourlet Transform and Local Energy Based Shape Histogram[C]. BICS, 2012, LNAI 7366, pp. 411–419

[6] A. Jafar, A.Q. Ikhlas, O. Jun-Seok, et al. Road Sign Detection and Shape recognition Invariant to Sign Defects[C]. Electro/Information Technology,2012 May,pp:1-6

[7] I. Sebanja, D.B. Megherbi. Automatic detection and recognition of traffic road signs for intelligent autonomous unmanned vehicles for urban surveillance and rescue[C]. IEEE International Conference on Technologies for Homeland Security, 2010 Nov,pp:132-138

[8] N. Barnes, G. Loy, D. Shaw. Regular polygon detection[C]. IEEE Conference Computer. Vision, 2005, pp. 778–785.

[9] B. Mohammed, C. Christophe, B. Michel et al. Triangular traffic signs detection based on RSLD algorithm[J]. Machine Vision and Applications 2013,24:1721–1732

[10] R. Belaroussi, J. Tarel. Angle vertex and bisector geometric model for triangular road sign detection[J]. Applications of Computer Vision,2009, pp:1–7

[11] S.Maldonado-Bascon, S. Lafuente-Arroyo, P. Gil-Jimenez,et al. Road-sign detection and recognition based on support vector machines[J]. Intelligent Transportation Systems, 2007, 8(2):264-278

[12] K.Jesmin, B. Sharif, A. Reza Hierarchical clustering of EMD based interest points for road sign detection[J]. Optics & Laser Technology,2013,57(2014) 271–283

[13] A. Ruta, Y. Li, and X. Liu, Towards real-time traffic sign recognition by class-specific discriminative features, BMVC, 2007,pp:399–408

[14] X.Baro, S.Escalera,J.Vitria,et al. Traffic sign recognition using evolutionary AdaBoost detection and forest-ECOC classification[J]. Intelligent Transportation Systems, 2009, 10(1): 113-126

[15] S.D. Zhu, Y. Zhang, X.F. Lu. Intelligent Approach for Triangle Traffic Sign Detection[J]. Journal of Image and Graphics, 2006,11(8):1127-1131

[16] H. Liu, D. Liu, J. Xin, Real-time recognition of road traffic sign in motion image based on genetic algorithm[C]. Machine Learning Cybern, 2002,pp:83-86

[17] Y. Ohta, T. Kanade, T. Sakai.Color information for region segmentation[J]. Computer Graph& Image Process,1980,13(2):224-241

[18] C.C. Chen. Improved Moment Invariants For Shape Discrimination[J]. Pattern Recognition,1993,26(5):683-686

TABLE II. COLOR AND SHAPE FEATURE OF TRAFFIC SIGNS SEGMENTATION

	Correct number	False-alarm number	Miss number	Correct rate	False-alarm rate	Miss rate
Paper[5]	138	5	4	93.9%	3.4%	2.7%
Paper[6]	124	11	12	84.4%	7.4%	8.2%
Proposed method	137	3	7	93.2%	2%	4.8%